J. Mater. Environ. Sci. 7 (3) (2016) 834-844 *Fitri et al.*
ISSN : 2028-2508
CODEN: JMESC

Theoretical studies of the master factors influencing the efficiency of thiazolothiazole-based organic sensitizers for DSSC

Asmae Fitri [a], Adil Touimi Benjelloun [a], Mohammed Benzakour [a], Mohammed Mcharfi [a], Mohammed Hamidi [b], and Mohammed Bouachrine [c]

[a] ECIM/LIMME, Faculty of sciences Dhar El Mahraz, University Sidi Mohamed Ben Abdallah, Fez, Morocco
[b]URMM/UCTA, FST Errachidia, University Moulay Ismaïl, Errachidia, Morocco
[c] ESTM, (LASMAR), University Moulay Ismaïl, Meknes, Morocco

Received 31 July 2015, Revised 23 Dec 2015, Accepted 04 January 2016
**For correspondence: Email:* bouachrine@gmail.com *(M. Bouachrine); Phone:* +212 5 35 73 31 71, +212 6 60 73 69 21*; Fax:* +212 5 35 73 31 71

Abstract

Four thiazolothiazole based dyes used for DSSCs with difference only in donor group were investigated via DFT and TDDFT approaches to shed light on how the π–conjugation order influence the performance of the dyes. Key parameters in close connection with the open-circuit photovoltage (V_{oc}) and the short-circuit current density (J_{sc}) including the light harvesting efficiency (LHE), injection driving force ($\Delta G^{inject.}$), reorganization energy (λ_{total}), vertical dipole moment ($\mu_{\perp}$), energy differences between E_{LUMO} and E_{CB} (V_{oc}) as well as the extent of electron recombination were discussed. The theoretical results reveal that all dyes can be used as potential sensitizers for TiO_2 nanocrystalline solar cells.

Keywords: DSSCs; thiazolothiazole; DFT; photovoltaic parameters; TiO_2 nanocrystalline solar cells.

1. Introduction

Dye Sensitized Solar Cells (DSSC) [1, 2] based on organic dyes adsorbed on nanocrystalline TiO_2 electrodes have attracted considerable attention in recent years because of their high incident solar light-to-electricity conversion efficiency and low cost of production [3]. A typical DSSC based on organic dyes is constructed with a wide band gap semi–conductor (typically TiO_2) sensitized with molecular dyes, electrolyte containing Iodide/triiodide (I^-/I_3^-) redox couple, and a platinum counter electrode [4]. The photochemical properties of different organic sensitizers have extensively been investigated in an attempt to design dyes with maximal visible light absorption coupled to long-lived excited states. However, major effort is still needed in both developing new sensitizers and finding optimal working conditions to improve the photon-to-current conversion efficiencies. At present, ruthenium complexes and metal porphyrins photosensitizers have an overall solar to energy conversion efficiency more than 12% for small area devices [5]. In view of the limited avaibility and environmental issues associated with ruthenium dyes, metal-free organic dyes are considered to be an alternative for use in DSSCs. Therefore, enormous progress has been made in this field, and several organic photosensitizers based on coumarin [6], indoline [7], carbazole [8], and triphenylamine [9] derivatives have been developed as promising candidates with the power conversion efficiency closing to ruthenium dyes. Up to now, the short-circuit current density (J_{sc}) and open-circuit photovoltage (V_{oc}) of metal-free organic dyes-based DSSCs are still lower than that of Ru(II)-based polypyridyl complexes. The main reason for this could be attributed to the relatively lower V_{oc} of organic DSSCs, arising from faster charge recombination rate and lower electron injection efficiency [10]. To further improve V_{oc} of DSSCs based on organic sensitizers, great efforts such as modifications on sensitizer, use of additives,

coadsorbents, novel redox couples, and tandem DSSCs have been made. The basic guidelines and strategies for improving V_{oc} have also been systematically discussed in Tian's review [11]. Given the key role of the sensitizer played in the cell, such as determining the light harvesting efficiency (LHE), the interfacial properties and the charge transfer process, there is no doubt that the modification on sensitizer is an effective way to enhance V_{oc} of the cell [11, 12]. However, the relationship between the sensitizer structure and V_{oc} is still unclear and intricate, although considerable experimental and theoretical studies have been conducted to resolve this problem in a trial and error way. Nonetheless, two important factors related to the sensitizer were considered to exert influences on the V_{oc} of the cell. One is the charge recombination dynamics through dye electrolyte interaction. For example, the relationship between dye-iodine interaction and cell voltage was investigated by Asaduzzaman et *al.* from the theoretical point [13] and by O'Regan et *al.* from the experimental point [14]. Miyashita et *al.* also demonstrated experimentally that the molecular structure of sensitizer and electrolyte could affect the interfacial electro-transfer kinetic in the DSSC [10]. The other is the TiO_2 conduction band energy shift (ΔE_{CB}) upon the sensitizer adsorption. Herein, we will account for both factors to design and screen efficient dyes by modulating dye/TiO_2/electrolyte interfacial interaction through DFT (Density Functional Theory) calculations, because there is no doubt that quantum chemical methods manifest themselves as a reliable and suitable avenue to rapid design and screen out efficient organic dyes reasonably, saving economical cost and synthesis efforts [15, 16].

The most extensively studied organic dyes usually adopt the donor–π spacer–acceptor (D–π–A) structural motif in order to improve the efficiency of the UV/Visible (UV/Vis) photoinducted intramolecular charge transfer (ICT). In this structure, the ICT from D to A at the photoexcitation will inject the photoelectron into the conduction band of the semiconductor through the electron accepting group at the anchoring unit. Considering lots of advantages of the thiazolothiazole as π–spacer [17–21] together the most commonly used cyanoacrylic acid acceptor, and the excellent electron donating ability of coumarin, indoline, carbazole and triphenylamine, we decided in this work to design new four organic D1, D2, D3 and D4 thiazolothiazole–based dyes. Figure 1a represents the optimized structures of these thiazolothiazole dyes used in this work and Figure 1b shows a simple dye-TiO_2 model [22-25] to simulate the interfacial interaction between the sensitizer and the semiconductor. It has been demonstrated that this simple model is appropriate for investigate geometries, electronic structures, and excitations of organic sensitizers after attaching to TiO2 surface [22, 25]. In this work, theoretical calculations on key parameters controlling the open-circuit photovoltage (Voc) and the short-circuit current density (Jsc) were performed to shed light on how and why the conjugation sequences of the donor group affect the performance of the dyes. And these parameters are: (i) light harvesting efficiency (LHE); (ii) injection driving force ($\Delta G_{inject.}$); (iii) reorganization energy (λ_{total}); (iv) the extent of charge recombination between the photoinjected electrons in the conduction band of semiconductor and the electron acceptors in the electrolyte, (v) vertical dipole moment ($\mu_{\perp}$); and (vi) energy differences between ELUMO and ECB (Voc). These theoretical criteria have been successfully used to evaluate the performance of the dyes used in DSSCs [22–24].

2. Computational Methods

All the calculations were performed with the Gaussian 09 packages [26]. The ground-state geometries of all organic dyes were optimized using density functional theory (DFT) with the hybrid functional B3LYP [27–29], coupled with the 6-31 G (d, p) basis set for C, H, O, N, S atoms, and a LANL2DZ basis set [30] which includes an effective core potential (ECP) for Ti atom. Frequency calculations were performed at the same level of theory as the optimizations to confirm the nature of the minima. Based on the optimized ground-state geometries, the UV-vis spectra of dyes were obtained by performing single-point time-dependent DFT (TDDFT) calculations with the long-range corrected CAM-B3LYP functional [31] with solvation effects included using an integral equation formalism polarizable continuum model (IEF–PCM) [32, 33]. The chloroform solvent was employed throughout this investigation. The cationic and anionic states of dyes were optimized at the B3LYP/6–31+G (d, p) level to calculate the total reorganization energies (λ_{total}). The natural bond orbital (NBO) analysis [34] was carried out at the B3LYP/6-31G(d, p) level for non-metal atoms and LANL2DZ level for Ti atom using NBO 3.1 program included in the Gaussian package program. To investigate dye-iodine intermolecular interaction, extra

DFT calculations were performed by the B3LYP functional using LANL2DZ basis set for I atom and 6-31G (d, p) basis set for other atoms.

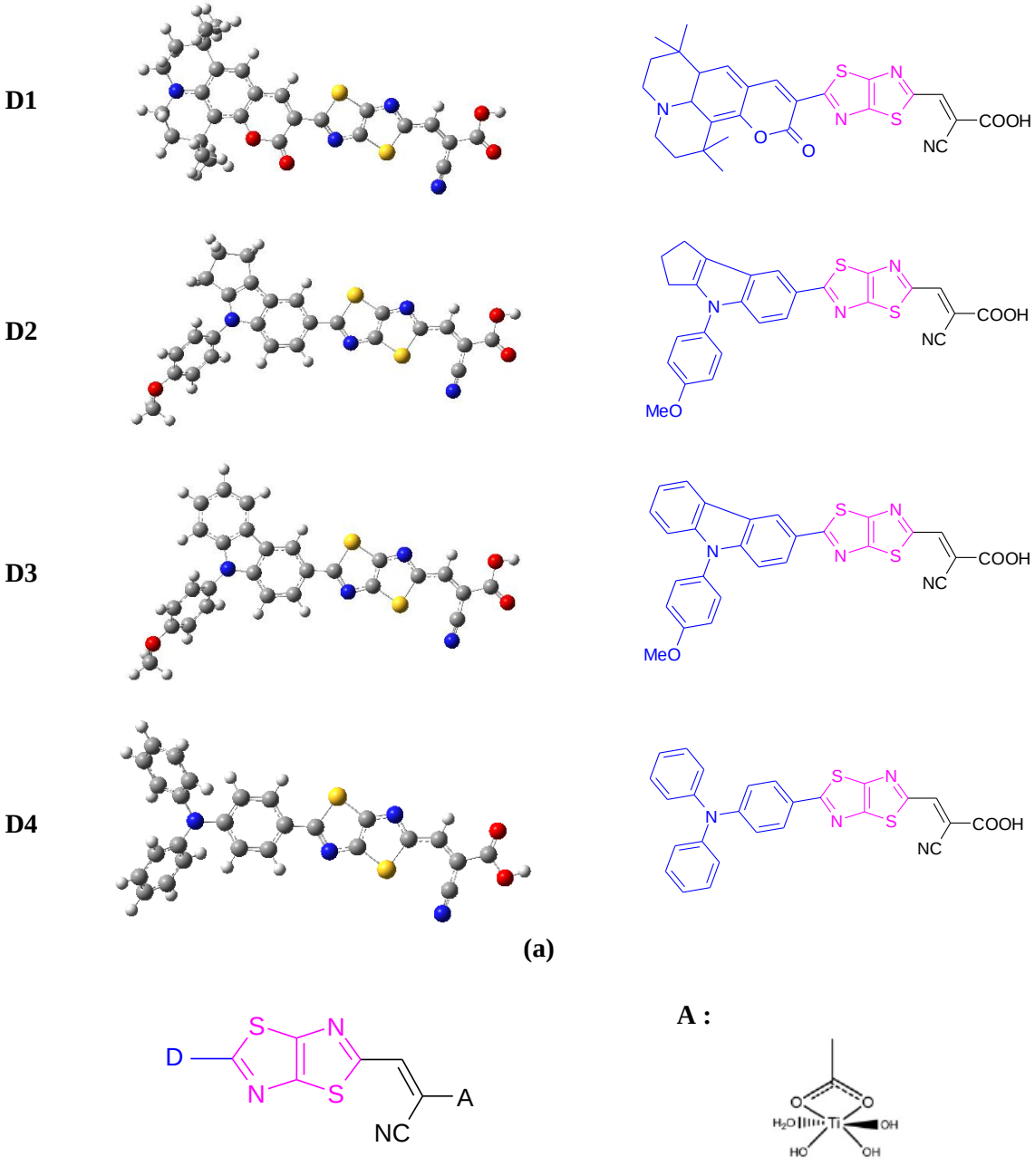

Figure 1: (a) Molecular structures of dyes D1-D4. (b) Simple model for all dyes binding on TiO_2 film (unit D are the donor groups in (a))

3. Results and discussion

3.1. Electronic absorption spectra

To gain insight of the optical property and electronic transition, the excitation energy and UV/Vis absorption spectra for the singlet–singlet transition of all sensitized dyes were simulated using TDDFT with CAM–B3LYP functional in chloroform solution before and after adsorption on TiO_2. Based on the previous works, the chloroform was used as solvent in the UV/Vis absorption spectra on the thiazolothiazole based molecules [17, 35]. The calculated data of maximum absorption wavelength, electronic vertical transition energy and oscillator strength of these dyes are summarized in Table 1a and Table 1b, and the corresponding simulated absorption spectra is shown in Figure 2.

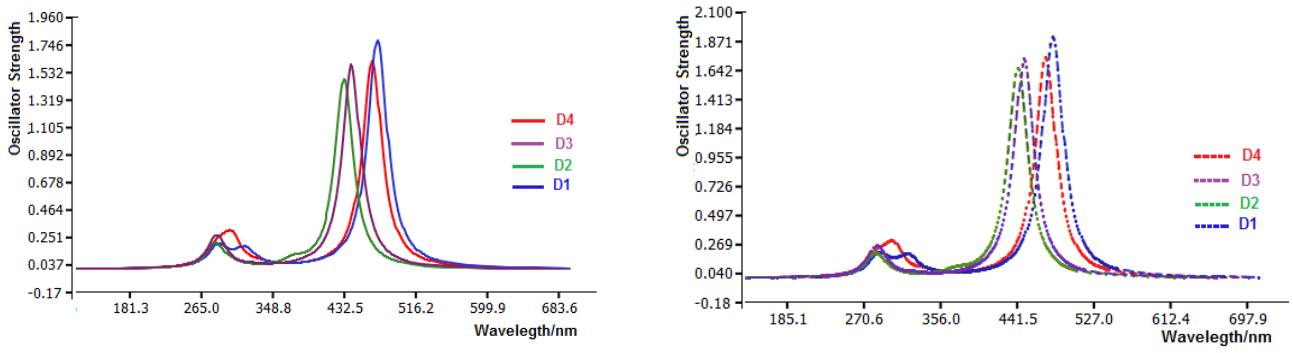

(a) **(b)**

Figure 2: Simulated absorption spectra in chloroform for all: **(a)** free dyes, **(b)** adsorbed dyes on TiO_2 film.

The computed results show that the strongest absorption peaks for all free dyes mainly related to the transition from the HOMO to LUMO. The maximum absorption are all blue-shift drastically, and the oscillator strength (*f*) are decreased by a large extent, to the detriment of the light capturing in the longer wavelength region. The spectra show similar profile for free dyes (Figure 2a) which presents a main intense band at higher energies from 433 to 472 nm, and was assigned to the ICT transitions. From Table 1a, we could find that as the donor group changing in free dyes, the first vertical excitation energies (*E*) were changed in decreasing order: D2>D3>D4>D1 showing that there is a red shift when passing from D2 to D1.

Table 1a. TD-CAM-B3LYP/6-31 G(d,p) computed absorption maxima (λ_{max}), excitation energies (*E*) and oscillator strengths (*f*) for free dyes in chloroform.

Dye	Main composition (HOMO=H, LUMO=L)	HOMO -1 (H-1)	HOMO (H)	LUMO (L)	*E* (eV)	λ_{max} (nm)	*f*
D1	H ⟶ L 0.61 H-1 ⟶ L 0.24	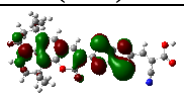	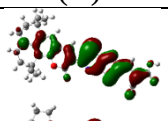	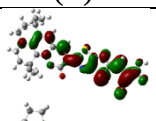	2.63	472.1	1.780
D2	H ⟶ L 0.41 H-1 ⟶ L 0.50	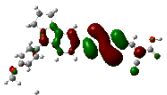	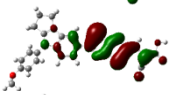	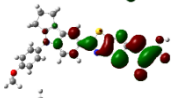	2.86	433.1	1.475
D3	H ⟶ L 0.61 H-1 ⟶ L 0.20	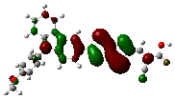	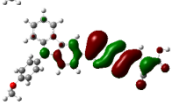	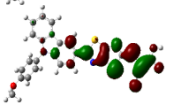	2.81	441.4	1.592
D4	H ⟶ L 0.62 H-1 ⟶ L 0.28	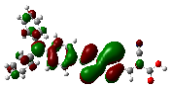	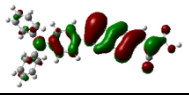	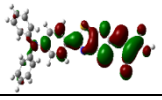	2.66	466.0	1.615

As we all know, the absorption spectrum properties could be affected when the dyes adsorb onto the semiconductor due to the interaction between them. Compared with the absorption properties of the free dyes, we prefer to get insight into the corresponding properties of the dyes after binding to semiconductor. Thus we also simulated the UV/Vis absorption spectra of the four dyes after binding to TiO_2 at the same level of theory for the free dyes except that the LANL2DZ basis set was used for Ti atom. The results are listed in Table 1b and Figure 2b. Apparently, after binding, the simulated optical spectra of the dye adsorbed onto the TiO_2 show similar profile where the maximum absorption wavelengths are red shifted, and *f* were improved due to the interaction between the dyes and the semiconductor comparing with the free dyes.

3.2. NBO analysis

In order to analyze the charge distribution and the electron–transfer mechanism of D–π–A dyes, the Natural Bond Orbital (NBO) analysis has been performed based on the optimized structure of the ground state (S_0) obtained at DFT/B3LYP/6–31G (d, p) level before and after binding on TiO_2.

Table 1b. TD-CAM-B3LYP/6-31 G(d,p) computed absorption maxima (λ_{max}), excitation energies (E) and oscillator strengths (f) for adsorbed dyes in chloroform.

Dye	Main composition (HOMO=H, LUMO=L)	HOMO -1 (H-1)	HOMO (H)	LUMO (L)	E (eV)	λ_{max} (nm)	f
D1	H ⟶ L 0.61 H-1 ⟶ L 0.25	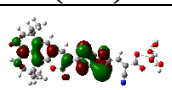	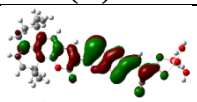	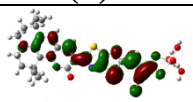	2.57	482.0	1.907
D2	H ⟶ L 0.41 H-1 ⟶ L 0.50	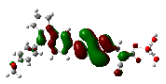	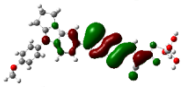	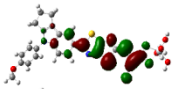	2.80	443.1	1.659
D3	H ⟶ L 0.61 H-1 ⟶ L 0.20	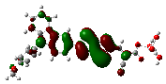	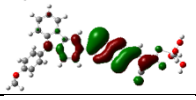	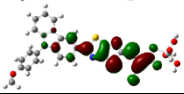	2.75	450.2	1.733
D4	H ⟶ L 0.62 H-1 ⟶ L 0.28	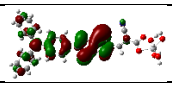		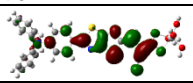	2.61	474.2	1.740

The electron donor units of the thiazolothiazole based dyes in this work are the coumarin, indoline, carbazole and triphenylamine, while the electronic acceptor is 2–cyanoacrylic acid. The calculated NBO charges that populated in the electron donor, conjugate bridge, electron acceptor groups and TiO_2 are listed in Table 2. Comparing the calculated NBO results of dyes D1–D4, the NBO charges of the electron donor are 0.176, 0.225, 0.219 and 0.223, respectively for free dyes, while they found 0.184, 0.248, 0.241 and 0.244, respectively for adsorbed dyes. The positive charges of the donor group of all dyes demonstrated they being an effective electron pushing unit. Contrarily, the negative charges in the π–conjugated linker and acceptor/anchoring group, shows that they are effective electron-pulling unit which trap the electron in the molecular backbone. During the photo–excitation, the electrons on the donor group of dyes are transferred to the acceptor group, and the charge separation state was formed in dyes. Furthermore, the NBO charges of the acceptor/anchoring group are prominent in the adsorbed dyes, especially for D2. That is, upon binding on the TiO_2 film, the electrons could be successfully transferred from the donor group to the acceptor group, finally injected into the conduction band of TiO_2.

Table 2: The natural bond orbital analysis (atomic charge) of the ground state of all dyes before and after adsorbed on TiO_2 film (in a.u.)

Dye	Free dyes			Adsorbed dyes			
	D	π	A	D	π	A	TiO_2
D1	0.176	-0.078	-0.098	0.184	-0.086	-0.538	0.441
D2	0.225	-0.117	-0.108	0.248	-0.103	-0.571	0.425
D3	0.219	-0.115	-0.104	0.241	-0.104	-0.559	0.386
D4	0.223	-0.117	-0.106	0.244	-0.114	-0.549	0.418

3.3. Factors influencing J_{sc}

3.3.1. Injection driving force

In order to better study the electrochemical properties of the dyes in their excited state, we introduce electron injection driving force $\Delta G^{inject.}$. We know that the electron injection efficiency Φ_{inject} could influence the short-circuit current density J_{sc}, which is closely related to the driving force of the electron injection from the photoinduced excited states of organic dyes to TiO_2 clusters surface. Consequently, we focus on the investigation of the injection driving force of the dyes in their excited state. It can be expressed as [36]:

$$\Delta G^{inject} = E^{dye*} - E_{CB} \quad (1)$$

where E^{dye*} is the oxidation potential energy of the dye in the excited state and E_{CB} is the reduction potential of the conduction band of TiO_2. There, we use in this work E_{CB} = –4.0 eV for TiO_2 [36], which is widely used in some papers [22–25]. There are two schemes to evaluate the E^{dye*} value, that is on the basis of the unrelaxed and relaxed geometries of the excited states by means of vertical and adiabatic excitation energy, respectively. However, it is justifiable to utilize the latter conveniently for future fast screening of photosensitizers, and there is also substantial experimental and theoretical evidence that the primary electron transfer event in DSSCs occurs

much faster than vibrational relaxation of the photoexcited dyes [22, 23]. In this case, E^{dye*} is estimated using unrelax path closer to the experimental value, and it can be estimated by [19–24,37]:

$$E^{dye*} = E^{dye} - E \quad (2)$$

where E^{dye} is the oxidation potential energy of the dye in the ground state, while E is an electronic vertical transition energy corresponding to λ_{max}. Based on Koopman's theorem, ground state oxidation potential energy is related to ionization potential energy. Thus, E^{dye} can be estimated as negative E_{HOMO} [38].

According to Eq. (1) and Eq. (2), the results of E^{dye} and deduced E^{dye*} and $\Delta G^{inject.}$ are displayed in Table 3. The theoretical results reveal that the electron donor significantly influences on E^{dye*}. We could find that for these dyes, they have negative $\Delta G^{inject.}$, implying that the electron injection process is spontaneous, and $-\Delta G^{inject.}$ is decreased in the order of D2(1.29 eV)>D4(1.28 eV)>D3(1.22 eV)>D1(1.12 eV), respectively. On the other hand, previous research has demonstrated that the driving force of –0.20 eV was necessary for efficient dye regeneration [39, 40].

Table 3: Estimated electrochemical parameters for all dyes.

Dye	E^{dye} (eV)	E^{dye*} (eV)	ΔG^{inject} (eV)	LHE	λ_h (eV)	λ_e (eV)	λ_{total} (eV)
D1	5.51	2.88	-1.12	0.98	0.24	0.39	0.63
D2	5.57	2.71	-1.29	0.97	0.20	0.35	0.55
D3	5.60	2.79	-1.22	0.97	0.18	0.34	0.53
D4	5.38	2.72	-1.28	0.98	0.12	0.45	0.57

3.3.2. Light harvesting ability

The light harvesting ability (LHE) and the electronic injection free energy ($\Delta G^{inject.}$) are the two main influencing factors on J_{sc}. To obtain a high J_{sc}, the efficient sensitizers applied in DSSCs should have a large LHE, which can be expressed as [41]:

$$LHE = 1 - 10^{-f} \quad (3)$$

where f is the oscillator strength of the dye associate to the wavelength λ_{max}. We noticed that the larger f obtained, the higher LHE will have. The LHE is a very important factor for the organic dyes considering the role of dyes in the DSSC, i.e. absorbing photons and injecting photoexcited electrons to the conduction band of the semi-conductor (TiO_2). In order to give an intuitional impression of how the donor groups affect the LHE, we simulated the UV/Vis absorption spectra of the four dyes. We could find that as the donor group changing, the oscillator strengths were changed slightly. As shown in Table 3, the LHE values for these dyes are in narrow range (0.97–0.98). This means that all the sensitizers give similar photocurrent.

3.3.3. Reorganization energy

As we know, besides LHE and $\Delta G^{inject.}$, the reorganization energy λ_{total} could also affect the kinetics of electron injection. So, the calculated λ_{total} is also important to analyze the relationship between the electronic structure and the J_{sc}. The small total reorganization energy (λ_{total}) which contains the hole and electron reorganization energy could enhance the J_{sc}. Namely, the smaller λ_{total} value obtained, the faster charge–carrier transport rates will be [41]. So we computed the hole and the electron reorganization energy (λ_h and λ_e) according to the following formula [42]:

$$\lambda_i = \left[E_0^{\pm} - E_{\pm}^{\pm}\right] + \left[E_{\mp}^{0} - E_0\right] \quad (4)$$

where $E_0^{\pm}$ is the energy of the cation or anion calculated with the optimized structure of the neutral molecule, $E_{\pm}^{\pm}$ is the energy of the cation or anion calculated with the optimized cation or anion structure, $E_{\pm}^{0}$ is the energy of the neutral molecule calculated at the cationic or anionic state, and the E_0 is the energy of the neutral molecule at ground state. As seen from Table 3, the calculated λ_{total} of all dyes are increased in the order: D3 (0.53 eV) < D2 (0.55 eV) < D4 (0.57 eV) < D1 (0.63 eV). The smaller λ_{total} value obtained the faster charge-carrier transport rates will be. Furthermore, balanced transport of both holes and electrons are important for high efficient DSSCs, that

is, the more balanced reorganization energy of hole and electron obtained, the more higher luminous efficiency will have [41, 42]. It distinctly shows that the differences between λ_h and λ_e of the designed dyes D1–D4 are 0.16, 0.15, 0.15 and 0.33 eV, respectively. Thus, the differences of D2 and D3 result in a more balanced transport rates than other D–π–A system investigated in this work. As a result, combining with the discussion of the electron injection driving force, light harvesting efficiency, and the reorganization energies of the studied organic dyes, we could predict that all dyes exhibit a favorable J_{sc} especially D2.

3.4. Factors influencing V_{oc}

We know that besides the short circuit current density (J_{sc}), the overall power conversion efficiency (η) could also be influenced by the open-circuit photovoltage (V_{oc}). In the following, we propose a reasonable measurement based on the issues related to V_{oc}. Upon the adsorption of dyes onto the semiconductor, the shift of E_{CB} could be expressed as [43]:

$$\Delta E_{CB} = -\frac{q\mu_{\perp}\gamma}{\varepsilon_0\varepsilon} \quad (5)$$

where q is the electron charge, $\mu_{\perp}$ is the component of dipole moment of the individual molecule perpendicular to the surface of semiconductor surface, γ is the dye's surface concentration, ε_0 and ε are the permittivity of the vacuum and the dielectric constant of the organic monolayer. Thus, according to Eq. (4), it is obvious that a dye with a large $\mu_{\perp}$ will induce a significant variation of V_{oc}. In this sense, we computed $\mu_{\perp}$to elucidate which dye might possesses relative larger V_{oc}. Considering the bidentate binding mode of the dyes, we made the C_2 axis of the carboxylate in the dye parallel to the x-axis, and the semiconductor surface is parallel to the yz plane (Figure 3). Table 4 summarized all computed results.

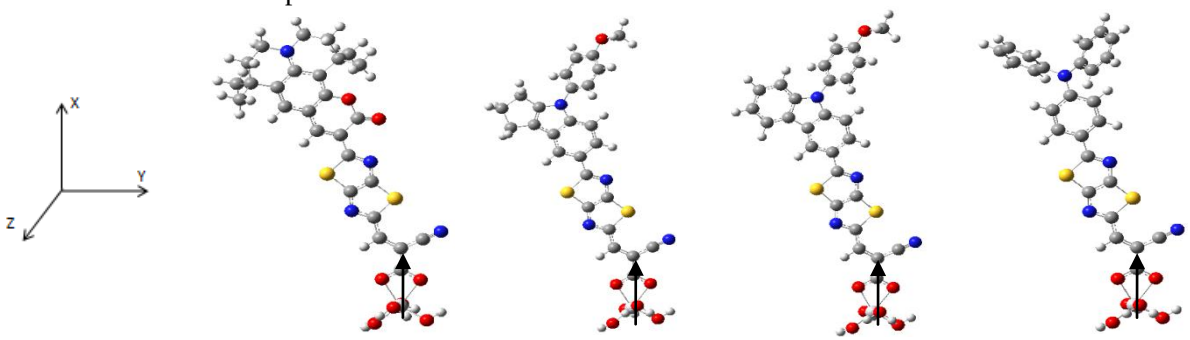

D1@TiO_2 13.30 D | D2@TiO_2 9.72 D | D3@TiO_2 8.62 D | D4@TiO_2 8.08 D

Fig. 3: Calculated vertical dipole moment of dyes adsorbed on TiO_2. The semiconductor surface is parallel to the yz plane.

Table 4: Critical parameters influencing V_{oc}.

Dye	$\mu_{\perp}$ /D	V_{oc}/eV	Atomic charge on the atom interacting with I_2 (in a.u.)	
			I_1-I_2	I_3-I_4
D1	13.30	0.97	-0.078	-0.039
D2	9.72	1.08	-0.080	-0.009
D3	8.62	1.02	-0.080	-0.061
D4	8.08	1.00	-0.079	-0.059

From Table 4, the $\mu_{\perp}$of these dyes decreased in the order of D1 (13.30 D) > D2 (9.72 D) > D3 (8.62 D) > D4 (8.08 D). In addition, V_{oc} can be approximately estimated by the energy difference between E_{LUMO} and E_{CB} in theoretically [37]:

$$V_{oc} = E_{LUMO} - E_{CB} \quad (6)$$

Certainly, it is obvious that the higher E_{LUMO} will cause a significant larger V_{oc}. Table 4 presents the calculated V_{oc} data. The computed change tendency followed by the decreased order: D2 (1.08 eV) > D3 (1.02 eV) > D4 (1.00 eV) > D1 (0.97 eV), respectively. It demonstrates that the LUMO energy level could influence the V_{oc}

remarkably. Thus, take the vertical dipole moment ($\mu_\perp$) and the difference value of E_{LUMO} and E_{CB} (V_{oc}) into account, dye D2 should exhibit the larger V_{oc} theoretically. On the other hand, a large $\mu_\perp$ and a suitable LUMO energy level could not guarantee always a high V_{oc} because the injected electron in the CB of the semiconductor could recombine with the redox couple (I^-/I_3^-) in the electrolyte and the oxidized organic dyes, and the former one is the main route of electron photovoltage losses [44-45]. The accepted knowledge is that the higher iodine concentration close to the TiO_2 surface, the shorter electron lifetime in the CB, which is related to lower V_{oc} values. Herein, to investigate the different molecular constructions effect on the recombination kinetics of the cell, we also investigated the dye–I_2 interaction by modeling the binding of I_2 to the various electron-donating sites in the dyes. Nitrogen, oxygen, and sulfur atoms in the organic dyes could form the halogen bonding through a non-covalent interaction, and the formation of dye–I_2 complex has also been reported in the experiment [46]. It is worth noting that I_3^- could also accept the electrons in the TiO_2 besides I_2, while Green et al. [45] have demonstrated that the rate of electron recombination with I_2 is two orders of magnitude faster than with I_3^-, thus here we consider I_2 as the main electron acceptor for electron combination in the electrolyte. The optimized molecular structures of the various adducts of dyes D1-D4 with I_2 and the distances of I-X (with X = N, O and S) are listed in Figure 4.

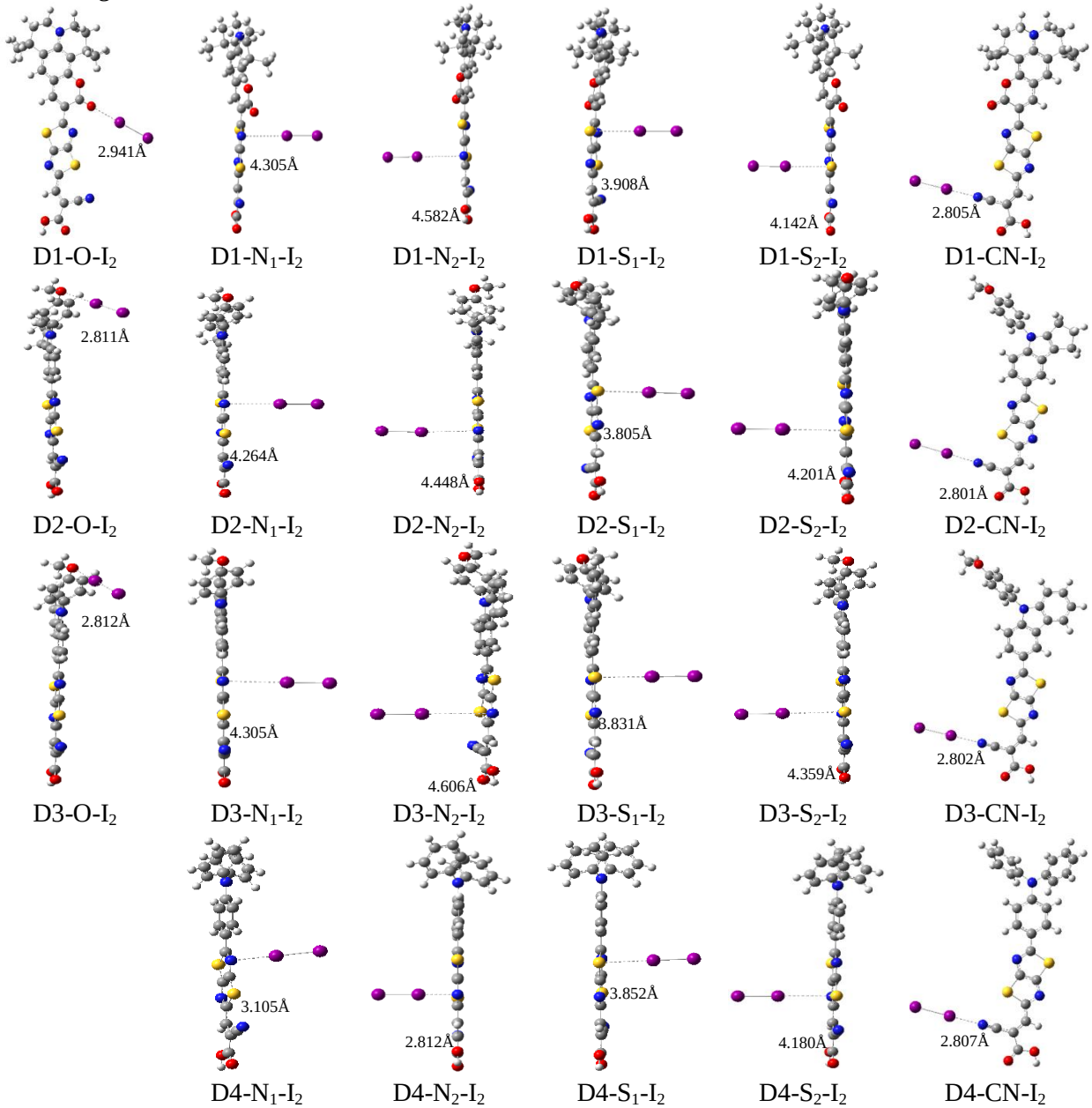

Figure 4: Geometries of the dyes–I_2 complex

It clearly depicts that I_2 preferred binding two sites for these dyes which are found to be at N of CN, O of donor group for D1-D3 and N of thiazolothiazole for D4 forming the halogen bonding through a non-covalent interaction. For these adducts, I_2 bonding through the N of the CN moiety are labeled as I_1–I_2, bonding through the O of the donor group or the N of the thiazolothiazole are labeled as I_3–I_4. It is obvious although the conjugation order changed, the most preferred binding site for each organic dye is the same, i.e. dye–CN–I_2 has the smallest distance for each dye as listed in Figure 4. The distances of the first preferred binding site at CN group (CN–I_2) are smaller than the net Van der Waals radii (3.53 Å) of the binding atoms, but larger than the net covalent radii (2.03 Å) [47]. At the same time, the second preferred binding site for dyes D1-D3 was found to be at donor group and at thiazolothiazole for D4, where the distances being significantly smaller than other binding sites. These results provide evidence that all the investigated dyes formed intermolecular charge-transfer complexes with I_2 indeed. Also, the distances of all binding sites in dyes D2 and D3 are significantly smaller than other dyes. Furthermore, the NBO analysis was carried out to obtain an initial evidence to explain the charge recombination mechanism. The corresponding calculations (Table 4) reflect that the negative atomic charges of I_2 in different electron-donating sites in dye–I_2 complex decreased in the order: D2<D1<D4<D3, that is, D2 possesses less electron donating sites with redox couple in the electrolyte which help to less electron losses. As noticed that, based on the $\mu_\perp$, V_{oc}, and electron recombination govern the photovoltage V_{oc} mostly, dye D2 is outstanding in all investigated dyes.

Conclusions

In this paper, we have designed a series of thiazolothiazole–based dyes containing different electron donors to obtain novel high performance dyes for DSSCs. The absorption spectra and electronic transition characteristics of designed systems were investigated by using DFT and TDDFT methods. We have discussed the key factors affecting the short-circuit current density (J_{sc}) and the open-circuit photovoltage (V_{oc}) of the cell including the light harvesting efficiency (LHE), injection driving force ($\Delta G^{inject.}$), reorganization energy (λ_{total}), vertical dipole moment ($\mu_\perp$), energy differences between E_{LUMO} and E_{CB} (V_{oc}), intermolecular interaction of dye–I_2 complexes as well as the NBO charges of dye-TiO_2 with the goal of finding potential sensitizers for use in DSSCs. It can be concluded that this class of selected thiazolothiazole dyes shows good photophysical properties related to DSSC use but in different outstanding properties. In summary, the theoretical results reveal that all dyes can be used as potential sensitizers for TiO_2 nanocrystalline solar cells because they possess high J_{sc} and V_{oc}, and thus the overall energy conversion efficiency would be improved. This theoretical approach presents a guiding tool to the synthesis process and helps to understand the structure–properties relationship of these new systems.

References

1. Grätzel M. Nature 414 (2001) 338.
2. Duncan W. R., Prezhdo O. V. *Annu. Rev. Phys. Chem*. 58 (2007) 143.
3. Mishra A., Fischer M. K. R., Bäuerle P., *Angew. Chem. Int. Ed.* 48 (2009) 2474.
4. Furube A., Katoh R., Yoshihara T., Hara K., Murata S., Arakawa H. et *al., J. Phys. Chem. B* 108 (2004) 12583.
5. Yella A., Lee H.W., Tsao H.N., Yi C.Y., Chandiran A.K., Nazeeruddin M.K., Diau E.W.G., Yeh C.Y., Zakeeruddin S.M., Gratzel M., *Science* 334 (2011) 629.
6. Wong B.M., Codaro J.G., *J. Chem. Phys.* 129 (2008) 214703.
7. Horiuchi T., Miura H., Sumioka K., Uchid S., *J. Am. Chem. Soc*. 126 (2004) 12218.
8. Srinivas K., Kumar C.R., Reddy M.A., Bhanuprakash K., Rao V.J., Giribabu L., *Synth Met* 161 (2011) 96.
9. Chunyang J., Zhongquan W., Jiaqiang Z., Zi L., Xiaojun Y., Yu S., *Spectrochim Acta A: Mol. Biomol. Spectrosc*. 86 (2012) 387.
10. Miyashita M., Sunahara K., Nishikawa T., Uemura Y., Koumura N., Hara K. et al., *J. Am. Chem. Soc.* 130 (2008) 17874.
11. Ning Z., Fu Y., Tian H., *Energy Environ. Sci.* 3 (2010) 1170.
12. Cui Y., Wu Y., Lu X., Zhang X., Zhou G., Miapeh F.B. et al., *Chem Mater* 23 (2011) 4394.
13. Asaduzzaman A.M., Chappellaz G.A.G., Schreckenbach G., *J Comput Chem* 33 (2012) 2492.
14. O'Regan B., Walley K., Juozapavicius M., Anderson A., Matar F., Ghaddar T. et al., *J Am Chem Soc* 131 (2009) 3541.
15. Martsinovich N., Troisi A., *Energy Environ Sci* 4 (2011) 4473.

16. Bourass M., Touimi Benjelloun A., Hamidi M., Benzakour M., Mcharfi M., Sfaira M. et *al.*, *J. Saud. Chem. Soc*. (2013), doi: http://dx.doi.org/10.1016/j.Jscs.2013.01.003
17. Ando S., Nishida J., Inohue Y., Tokito S., Yamashita Y., *J. Mater Chem.* 14 (2004) 1787.
18. Subramaniyan S., Xin H., Kim F.S., Shoaee S., Durrant J.R., Jenekhe S.A., *Adv. Energy Mater* 1 (2011) 854.
19. Fitri A., Touimi Benjelloun A., Benzakour M., Mcharfi M., Sfaira M., Hamidi M., Bouachrine M., *Res. Chem. Interm*. 39 (2013) 2679.
20. Fitri A., Touimi Benjelloun A., Benzakour M., Mcharfi M., Hamidi M., Bouachrine M., **Spectrochim. Acta A: Mol. Biomol. Spectrosc.** 124 (2014) 646.
21. Fitri A., Touimi Benjelloun A., Benzakour M., Mcharfi M., Hamidi M., Bouachrine M. Spectrochim. Acta A: Mol. Biomol. Spectrosc. 132 (2014) 232.
22. Preat J., Jacquemin D., Michaux C., Perpète E.A., *Chem. Phys*. 376 (2010) 56.
23. Zhang J., Li H.B., Sun S.L., Geng Y., Wu Y., Su Z.M., *J. Mater Chem*. 22 (2012) 568.
24. Liu D.S., Ding W.L. , Zhu K.L., Geng Z.Y., Wang D.M., Zhao X.L., *Dyes Pigm.* 105 (2014) 192.
25. Agrawal S., English N.J., Ravindranathan T.K., MacElroy J.M.D., *Phys. Chem. Chem. Phys* 14 (2012) 12044.
26. Frisch M.J., Trucks G.W., Schlegel H.B., Scuseria G.E., Robb M.A., Cheeseman J.R. et *al.* Gaussian 09, revision A.02. Pittsburgh PA: Gaussian, Inc; (2009).
27. Becke A.D., *J. Chem. Phys.* 98 (1993) 1372.
28. Becke A.D., *Phys. Rev. A* 38 (1988) 3098.
29. Lee C., Yang W., Parr R.G., *Rev. B* 37 (1988) 785–89.
30. Yao B.Q., Sun J.S., Tian Z.F., Ren X.M., Gu D.W., Shen L.J., et *al*. *Polyhedron* 27 (2008) 2833.
31. Yanai T., Tew D.P., Handy N.C. *Chem. Phys. Lett.* 393 (2004) 51.
32. Cossi M., Barone V. *J. Chem. Phys.* 115 (2001) 4708.
33. Adamo C., Barone V. *Chem. Phys. Lett.* 330 (2000)152.
34. Foster J.P., Weinhold F. *J. Am. Chem. Soc*. 102 (1980)7211.
35. Hu C., Wu Z., Cao K., Sun B., Zhang Q. *Polymer* 54 (2013) 1098.
36. Asbury J.B., Wang Y.Q., Hao E., Ghosh H., Lian T. Res. Chem. Intermed. 27 (2001) 393.
37. Sang–aroon W., Saekow S., Amornkitbamrung V. *J. Photochem. Photobiol.* A 236 (2012) 35.
38. Pearson R.G. *Inorg. Chem*. 27 (1988) 734.
39. Zhu W., Wu Y., Wang S., Li W., Li X., Chen J., et *al*. *Adv. Funct. Mater* 21 (2011) 756.
40. Hara K., Sato T., Katoh R., Furube A., Ohga Y., Shinpo A., et *al*. J. *Phys. Chem. B* 107 (2003) 597.
41. Zhang Z.L., Zou L.Y., Ren A.M., Liu Y.F., Feng J.K., Sun C.C. *Dyes Pigm*. 96 (2013) 349.
42. Balanay M.P., Kim D.H. *J. Mol. Struct. (Theochem)* 910 (2009) 20.
43. Chen P., Yum J.H., Angelis F.D., Mosconi E., Fantacci S., Moon S.J. et *al*. *Nano. Lett* 9 (2009) 2487.
44. Liu J., Zhou D., Wang F., Fabregat-Santiago F., Miralles S.G., Jing X., Bisquert J., Wang P. J. *Phys. Chem*. C 115 (2011) 14425.
45. Green A.N.M., Palomares E., Haque S.A., Kroon J.M., Durrant J.R. *J. Phys. Chem. B* 109 (2005) 12525.
46. Tuikka M., Hirva P., Rissanen K., Korppi-Tommola J., Haukka M. *Chem. Comm* 47 (2011) 4499.
47. Kusama H., Sugihara H., Sayama K., *J. Phys. Chem.* C 115 (2011) 9267.